STRENGTH PREDICTION AND EXPERIMENTAL VALIDATION OF ADHESIVE JOINTS INCLUDING POLYETHYLENE, CARBON-EPOXY AND ALUMINIUM ADHERENDS

A. M. G. Pinto[1,a], A. G. Magalhães[1,b], R. D. S. G. Campilho[2,c], M. F. S. F. de Moura[2,d], A. P. M. Baptista[2,e]

[1] ISEP, Instituto Superior de Engenharia do Porto, R. Dr. António Bernardino de Almeida, 431, 4200-072 Porto, Portugal

[2] FEUP, Faculdade de Engenharia da Universidade do Porto, R. Dr. Roberto Frias, s/n, 4200-465 Porto, Portugal

[a]agp@isep.ipp.pt, [b]agm@isep.ipp.pt, [c]raulcampilho@hotmail.com, [d]mfmoura@fe.up.pt, [e]amb@fe.up.pt

Keywords: Polyethylene, Polypropylene, acrylic adhesives, single lap adhesive joints, mechanical strength.

Abstract. Polyolefins are especially difficult to bond due to their non-polar, non-porous and chemically inert surfaces. Acrylic adhesives used in industry are particularly suited to bond these materials, including many grades of polypropylene (PP) and polyethylene (PE), without special surface preparation. In this work, the tensile strength of single-lap PE and mixed joints bonded with an acrylic adhesive was investigated. The mixed joints included PE with aluminium (AL) or carbon-fibre reinforced plastic (CFRP) substrates. The PE substrates were only cleaned with isopropanol, which assured cohesive failures. For the PE-CFRP joints, three different surfaces preparations were employed for the CFRP substrates: cleaning with acetone, abrasion with 100 grit sand paper and peel-ply finishing. In the PE-AL joints, the AL bonding surfaces were prepared by the following methods: cleaning with acetone, abrasion with 180 and 320 grit sand papers, grit blasting and chemical etching with chromic acid. After abrasion of the CFRP and AL substrates, the surfaces were always cleaned with acetone. The tensile strengths were compared with numerical results from ABAQUS® and a mixed-mode (I+II) cohesive damage model. A good agreement was found between the experimental and numerical results, except for the PE-AL joints, since the AL surface treatments were not found to be effective.

Introduction

Polyolefins are being increasingly used in industry due to their properties and reduced cost. However, bonding of these low surface energy polymers tend to be more expensive than for many other plastics. Actually, polyolefins are very difficult to bond due to their non polar, non porous and chemically inert surfaces. Traditionally, surface preparation or pre-treatment are necessary to properly bond this kind of materials. Chemical etching, flame treating, corona discharge, plasma etching, UV irradiation or chemical primers are amongst the most common pre-treatments [1-2]. Nevertheless, these pre-treatments render the process slow, expensive and, consequently, less attractive to industry. Fortunately, the on-going development of adhesive technology made easier to bond these materials. Acrylic adhesives were recently introduced, particularly adapted to join these materials without special surface preparation. The resulting bonds are structural and can replace screws, rivets, plastic welding, and processes that include surface treatments. The pre-treatment time and associated costs are eliminated. An interesting characteristic of acrylic adhesives is the possibility to bond plastics to other materials, such as metal, composites and glass. Pot-life time can vary from 2 to 15 minutes, permitting the alignment and repositioning of the components. These

adhesives can also be robotically applied. The widespread application of adhesive bonds with these materials justifies the development of accurate predictive tools.
In this study, the tensile strength of single-lap PE and mixed joints bonded with an acrylic adhesive was evaluated. PE-PE, PE-CFRP and PE-AL joints were investigated. Experimentally, the influence of several surface treatments for the AL and CFRP substrates on the joints strength was assessed. These included chemically etching, grit blasting and abrading with sandpaper. The joint strengths were compared with numerical ones using ABAQUS® and a mixed-mode cohesive damage model, based on the indirect use of Fracture Mechanics and implemented within cohesive elements. A good agreement was found between the experimental and numerical results.

Experimental work

Adhesively-bonded single-lap joints were used in this study. Different substrate materials were considered: PE (PE500), CFRP prepreg (Texipreg HS160RM from SEAL®) and AL (AW6063-T6). Young's modulus (E) of 1000 MPa and Poisson's ratio (ν) of 0.3 were considered for the simulations of the PE substrates. The structural acrylic adhesive 3M DP-8005® was used (E=590 MPa and ν=0.35). The experimentally measured values of E=67 GPa and ν=0.35 were employed for the aluminum substrates. The orthotropic elastic properties of a CFRP ply are shown in Table 1 (1 denotes the fibres direction, 2 the transverse direction and 3 the thickness direction).

Table 1 – Carbon-epoxy ply orthotropic elastic properties [3].

E_1=1.09E+05 MPa	ν_{12}=0.342	G_{12}=4315 MPa
E_2=8819 MPa	ν_{13}=0.342	G_{13}=4315 MPa
E_3=8819 MPa	ν_{23}=0.380	G_{23}=3200 MPa

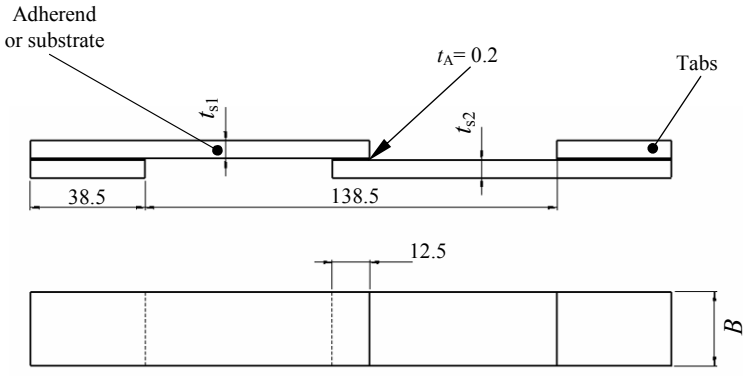

Fig. 1 – Single-lap joint geometry (dimensions in mm).

The PE substrates were only cleaned with isopropanol. With this method cohesive failures were guaranteed to occur [4]. In the PE-CFRP joints, three different surfaces preparations were selected for the CFRP substrates: cleaning with acetone, abrading with 100 grit sand paper and peel-ply finishing. The ply was removed prior to bonding and then the surfaces were cleaned with acetone. In the PE-AL joints, the AL bonded surfaces were prepared by the following methods: cleaning with acetone, abrasion with 180 and 320 grit sand papers, grit blasting and chemical etching with chromic acid. After all of these treatments, the surfaces were cleaned with acetone. The joints strength was determined by the Lap Shear Test Method (ASTM D3163 and ASTM D1002). However, depending on the substrate material, different thicknesses were considered to avoid substrate failures. The joint geometry is shown in Fig. 1. Table 2 presents the dimensions of each substrates combination. The value of t_A was fixed at 0.2 mm with glass micro spheres mixed with the adhesive. The adhesive excess at the overlap edges was removed in all joints. Pressure was applied to the lap joint during the curing cycle by one spring clamp. The joints bonding and

assembly was accomplished with an especially manufactured tool, allowing the standardized joint preparation technique to be used repeatedly. Tabs were bonded at the joints edges to assure a correct alignment in the testing machine (Fig. 1). The specimens were left at ambient conditions for one week prior to testing.

Table 2 – Substrates dimensions for each combination (dimensions in mm).

Sub. 1-Sub. 2	Substrate 1		Substrate 2	
	Thickness (t_{s1})	Width (B)	Thickness (t_{s2})	Width (B)
PE-PE	6	25	6	25
PE-CFRP	6	15	1.2	15
PE-AL	6	25	3	25

The joints were tested in an Instron 4208 testing machine, equipped with a 5 kN load cell and under displacement control (1.3 mm/min). The average shear strength was calculated as the measured peak load divided by the bonded area. The test values in this work are an average of at least five measurements. The failure modes were characterized by visual inspection, after failure. Plasticization only occurred in the PE substrates. Consequently, bulk tests were conducted on this material. The P-δ curve with be later on introduced in the simulations, to account for these effects.

Cohesive Damage Model

A mixed-mode (I+II) cohesive damage model implemented within zero thickness cohesive elements was used to simulate damage initiation and propagation. A triangular law between stresses ($\boldsymbol{\sigma}$) and relative displacements ($\boldsymbol{\delta}_r$) was used (Fig. 2).

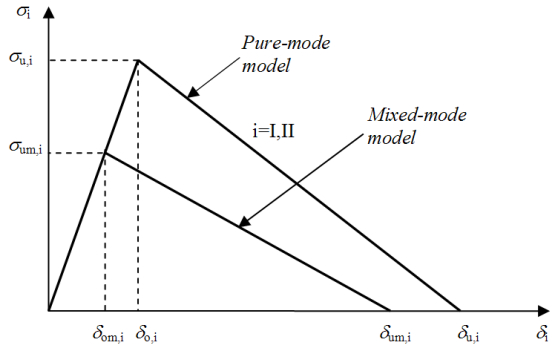

Fig. 2 – The triangular constitutive law for pure-mode and mixed-mode.

It is thus necessary to know the local strength at the crack tip ($\sigma_{u,i}$, i=I, II) and the fracture toughness (G_{ic}, i=I, II) in each mode. Damage initiation is predicted using the quadratic stress criterion

$$\begin{aligned} &\left(\frac{\sigma_{\mathrm{I}}}{\sigma_{\mathrm{u,I}}}\right)^2+\left(\frac{\sigma_{\mathrm{II}}}{\sigma_{\mathrm{u,II}}}\right)^2=1 \quad \text{if} \quad \sigma_{\mathrm{I}}>0 \\ &\sigma_{\mathrm{II}}=\sigma_{\mathrm{u,II}} \qquad\qquad\quad \text{if} \quad \sigma_{\mathrm{I}}\le 0 \end{aligned}, \tag{1}$$

where σ_i, (i=I, II) corresponds to the stress in a given integration point of a cohesive element in the respective pure mode. Damage growth is predicted using the linear energetic criterion

$$\frac{G_{\mathrm{I}}}{G_{\mathrm{Ic}}}+\frac{G_{\mathrm{II}}}{G_{\mathrm{IIc}}}=1\,. \tag{2}$$

The area under the minor triangle of Fig. 2 represents the energy released in each mode, while the bigger triangle area corresponds to the respective G_{ic}. When equation (2) is satisfied, damage propagation occurs and stresses are completely released, with the exception of normal compressive ones. A detailed description of the model used is presented in the work of Campilho et al. [5].

Numerical models

The numerical analyses including the cohesive damage model presented previously were carried out in ABAQUS®. A non-linear material and geometrical analysis was performed using plane-stress 8-node rectangular solid finite elements. Fig. 3 shows a mesh detail of the PE-PE joint at one end of the overlap. The cohesive elements are represented by the small crosses, being employed at the substrate/adhesive interfaces and at the middle of the adhesive thickness.

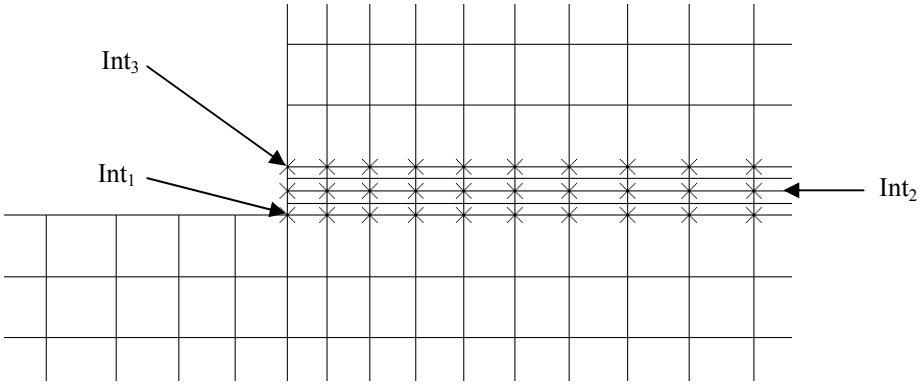

Fig. 3 – Detail of the mesh used for the PE-PE joint at one end of the overlap.

Sixteen elements were used along the substrates thickness, and forty elements were employed along the overlap. Furthermore, biasing effects were used, allowing for a more refined mesh where stress gradients are known to be greater, i.e., the overlap edges [3]. Boundary conditions intended to replicate the experimental tests. Thus, one of the joint edges was clamped, and the other was restrained in direction y and subjected to a tensile displacement. The displacement was applied incrementally up to failure and the P-δ curves extracted. The complete σ-ε curve of the PE was introduced in the numerical models. The AL and CFRP substrates were modelled as linear elastic materials, using the elastic properties mentioned, since no plastic deformations were detected experimentally after the specimens failure.

Results

The average experimental strengths and respective standard deviations for the joints with different substrate combinations and surface preparations are showed in Fig. 4. The numerical strengths are also included. Table 3 details the surface preparation for each set of joints and the respective failure modes observed. Experimentally, the best results were obtained with the PE-CFRP joints, with identical values for the acetone cleaning and sand paper abrasion surface preparation techniques (approximately 8 MPa). Slightly smaller values were obtained for the peel ply finishing. The authors attribute this difference to the minor adhesive failure regions in the CFRP. In the PE-PE joints, slightly smaller strengths were obtained. This difference is imputable to the higher joint bending for the PE-PE joints. The values of E for plastics are smaller, when compared to metals and composites. Consequently, the PE-PE joints suffer considerable bending during testing (Fig. 5), which introduces peel stresses on the joints and reduces their strength [6]. The worst results were obtained for the PE-AL joints, with a maximum strength of 6.07 MPa for the joints with grit blasted aluminium substrates. The partially adhesive failures observed in the aluminium substrates substantiate the difference to the other joints. For the other surface treatments on the AL substrates,

practically adhesive failures justify a further strength reduction.

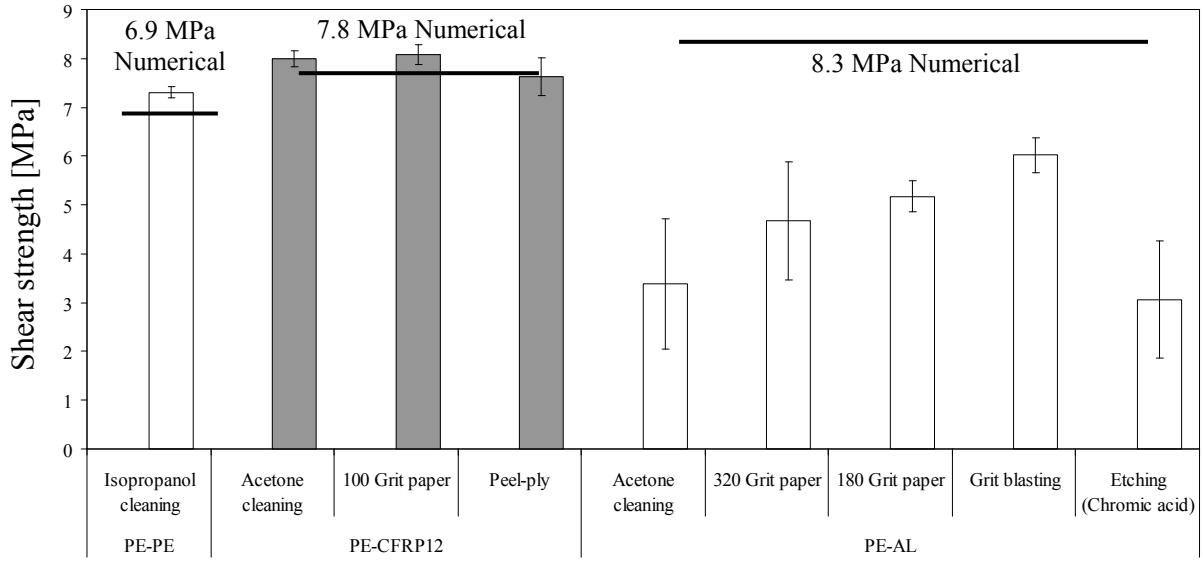

Fig. 4 – Numerical and experimental shear strengths as a function of the substrates combinations and surface preparation techniques.

The large scatter in the PE-AL results is due to different adhesive failure/cohesive failure ratios between specimens of the same set. In fact, higher cohesive failure percentile areas yielded higher shear strengths. Owing to these results, the authors conclude that the surface treatments evaluated on the aluminium substrates are not appropriate for the adhesive under analysis, since a weaker AL\adhesive layer interface is achieved, compared to the adhesive layer cohesive strength.

Table 3 – Failure modes in the single-lap shear tests.

Joint	Surface preparation	Failure mode
PE-PE	Cleaned by isopropanol	Cohesive failure
PE-CFRP	PE: cleaned with isopropanol CFRP: cleaned with acetone	Cohesive failure and interlaminar failure of the CFRP substrate
	PE: cleaned with isopropanol CFRP: 100 grit paper	Cohesive failure and interlaminar failure of the CFRP substrate
	PE: cleaned with iopropanol CFRP: peel-ply	Cohesive failure and adhesive failure of the CFRP substrate
PE-AL	PE: cleaned with isopropanol AL: cleaned with acetone	Predominantly adhesive failure on the aluminium substrate, very small cohesive regions
	PE: cleaned with isopropanol AL: 320 grit paper	Predominantly adhesive failure on the aluminium substrate, very small cohesive regions
	PE: cleaned with isopropanol AL: 180 grit paper	Predominantly adhesive failure on the aluminium substrate, small cohesive regions
	PE: cleaned with isopropanol AL: grit blasting	Mixed failure (cohesive failure and adhesive failure on the aluminium substrate)
	PE: cleaned with isopropanol AL: chromic acid	Predominantly adhesive failure on the aluminium substrate, very small cohesive regions

The numerical analyses were in good agreement with the experiments for the PE-PE and PE-CFRP joints (Fig. 4), showing cohesive experimental fractures. The deviation for the PE-AL joints is caused by the experimental adhesive failures. In fact, the cohesive damage model assumes cohesive properties of the adhesive for all cohesive elements (Int_1, Int_2 and Int_3 in Fig. 3), which is not consistent with the test results in this particular configuration. The numerical results show a higher strength for the PE-AL joints, since with this substrate combination the joint bending and consequent peel stresses are significantly smaller (Fig. 5), increasing the joint strength. The numerical P-δ curves (not presented in this article) simulated with an acceptable accuracy the joints

behaviour. However, a slight deviation was observed between the shape of the experimental and numerical curves, explained by the ductility of the adhesive used, following an approximate trapezoidal shape instead of immediate softening after attaining the peak strength [6].

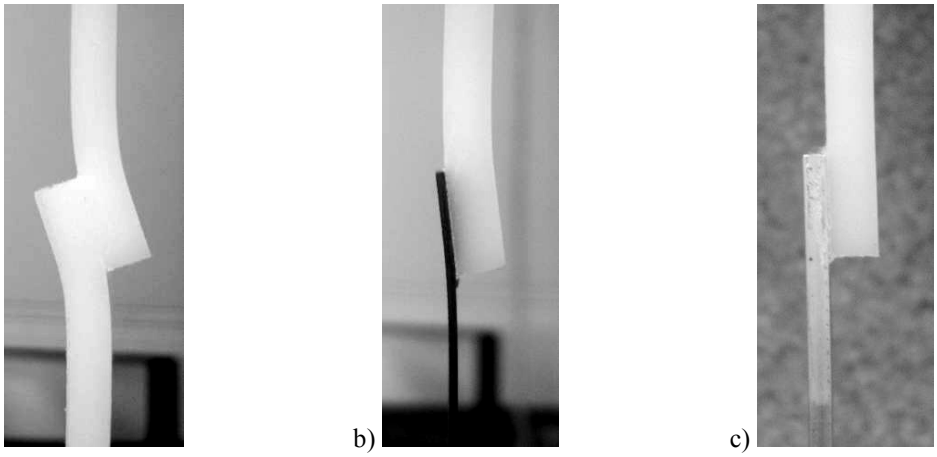

Fig. 5 – Deformed shape of the PE-PE (a), PE-CFRP (b) and PE-AL (c) joints before failure.

Summary

The strength of single-lap joints bonded with an acrylic adhesive was evaluated for PE-PE, PE-CFRP and PE-AL substrates. Experimentally, the highest strength was achieved with the PE-CFRP joints, followed by the PE-PE joints. The slight strength reduction for these last was justified by the higher joint bending, increasing peel stresses in the adhesive layer. Significant lower strengths were obtained for the PE-AL joints, due to the inadequacy of the surface preparation techniques employed, resulting in partially adhesive failures. The joints fracture was simulated using a mixed-mode cohesive damage model implemented within cohesive elements. A good agreement was found between the experimental and numerical failure loads. However, for the PE-AL joints the strengths were overestimated, since in the experiments failures were partially adhesive. Overall, the authors concluded that the numerical models are adequate to simulate the behaviour of these joints. On the adequacy of the acrylic adhesive tested to bond the materials analysed in this work, it is emphasized that cleaning the substrates guarantees a cohesive failure for the polyethylene and CFRP. For the aluminium substrate, the surface preparation techniques evaluated were insufficient to achieve a good adhesion and, consequently, cohesive failures.

References

[1] M.D. Green, F.J. Guild and R.D. Adams: Int. J. Adhes. Adhes. Vol 22 (2002), p. 81.

[2] S. Bhowmik, T.K. Chaki, S. Ray, F. Hoffman and L. Dorn: Int. J. Adhes. Adhes. Vol. 24, (2004), p. 461.

[3] R.D.S.G. Campilho, M.F.S.F. de Moura and J.J.M.S. Domingues: Compos. Sci. Technol. Vol. 65 (2005), p. 1948.

[4] A.M.G. Pinto, A.G. Magalhães, F.G. da Silva and A.P.M. Baptista: Int. J. Adhes. Adhes. Vol. 28 (2008), p. 452.

[5] R.D.S.G. Campilho, M.F.S.F. de Moura and J.J.M.S. Domingues: J. Adhes. Sci. Technol. Vol. 21 (2007), p. 855.

[6] A.M.G. Pinto, A.G. Magalhães, R.D.S.G. Campilho, M.F.S.F. de Moura, A.P.M. Baptista: Accepted in J. Adhesion.